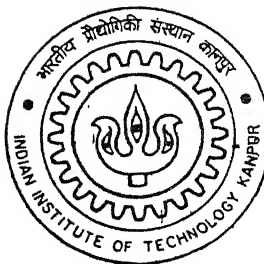


MODELLING OF PERFORMANCE OF AN ARTILLERY ROCKET USING NEURAL NETWORKS

By
Om Prakash

TH
AE/2001/M
Om Gm



DEPARTMENT OF AEROSPACE ENGINEERING
Indian Institute of Technology Kanpur
DECEMBER, 2001

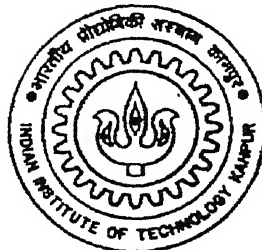
MODELLING OF PERFORMANCE OF AN ARTILLERY ROCKET USING NEURAL NETWORKS

A Thesis Submitted
in Partial Fulfillment of the Requirements
for the Degree of

Master of Technology

by

Om Prakash



to the

**Department of Aerospace Engineering
Indian Institute of Technology, Kanpur**

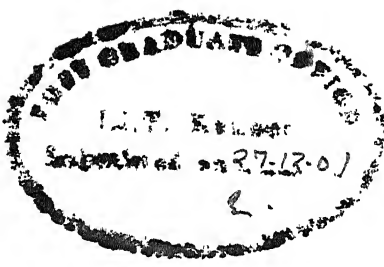
December, 2001

2017-2018/AE
गोपनीय अधिकारी का नाम
प्रतिवर्ष अधिकारी का नाम
क्रमांक संख्या 137901



A137901

CERTIFICATE



It is certified that the work contained in this thesis entitled, "**Modelling of Performance of an Artillery Rocket using Neural Networks**" by Om Prakash has been carried out under my supervision and that this work has not been submitted elsewhere for a degree.



(Dr. A. K. Ghosh)

Assistant Professor

Department of Aerospace Engineering

Indian Institute of Technology

Kanpur - 208016

December, 2001

ABSTRACT

In recent times, the most widely used trajectory modelling for artillery rockets has been via mathematical models such as point mass model, modified point mass model and six-degrees-of-freedom model. Application of these models require an a priori postulation of equations of motion governing the rocket trajectory and to solve these equations, one need reliable estimates of aerodynamic coefficients, exact values of initial conditions (at launch). Due to various assumptions and approximations used in arriving at the mathematical model (trajectory model) and also due to non-availability of reliable estimates of aerodynamic coefficients, initial conditions required to solve these equations, an alternate approach of using general function approximation capability of the feed forward neural networks (FFNNs) for estimating rocket performance in terms of range and drift is explored. Range is the axial distance traversed by the rocket along the line of fire, whereas drift represents the lateral-deviation from the line of fire. The present work addresses this aspect of estimating rocket performance by way of proposing three distinct neural models for predicting trajectory variables.

To start with, the present work addresses the problems associated with conventional model to predict trajectory performance of rockets. Finally, it proposes three distinct neural model, using FFNNs for predicting trajectory variables. These models are validated for Grad Rocket data supplied in the form of range tables by ARDE, Pune. The estimated trajectory parameters like the range (R), the firing angle (θ) drift (ψ), etc. via the proposed neural models compare well with those listed in the supplied range table. The neural models developed take into account variations in atmospheric

conditions like head/tail wind, cross wind, charge temperature, ambient temperature and pressure that might prevail at the time of firing. It is shown that the proposed models can accurately predict i) the range obtainable for varying firing angles and prevailing atmospheric conditions, charge temperature, ii) the firing angle required to achieve desired range for known atmospheric conditions, charge temperature and, iii) the standard range that the rocket would have achieved under standard atmospheric conditions.

ACKNOWLEDGEMENTS

With a profound sense of gratitude, I express my sincere thanks to my esteemed teachers and thesis supervisor, Dr. A. K. Ghosh for their invaluable guidance and encouragement throughout this work. I am indebted to them for providing me with all the required facilities and help in every possible way at IIT Kanpur. I also express my sincere thanks to Dr. S. C. Raisinghani for his invaluable suggestions during entire course of this work. I also express my sincere thanks to Mr. Ankur Singhal (Research Associate) for his timely help in modelling and data analysis. But for their untiring cooperation, time and patience, this work would not have seen the light of the day.

I would like to thank “BHARAT VIKAS PARISHAD” society for financially helping me during my admission of M.Tech. program.

I have no words to express my thanks to my parents, brothers and sister, who have been a constant source of moral encouragement and inspiration to me.

I wish to thank all my friends and well wishers who made my stay at IIT Kanpur, memorable and pleasant.

Om Prakash

CONTENTS

ABSTRACT	iii
LIST OF FIGURES	vii
LIST OF TABLES	viii
NOMENCLATURE	ix
1 Introduction	1
2 Artificial Neural Network	6
2.1 Introduction	6
2.2 Back Propagation Algorithm	7
3 Trajectory and Range Modelling of Artillery Rocket	11
3.1 General	11
3.2 The Point mass model	11
3.3 The six-degrees-of-freedom model	12
3.4 Range tables for Grad-Rocket	16
4 Neural models, Results and Discussion	20
4.1 Analysis of Grad-Rocket	20
4.2 Modelling of Rocket trajectory using six degrees of freedom trajectory model	23
4.3 Neural Modelling	33
4.4 Model 1	35
4.5 Model 2	38
4.6 Model 3	41
5. Conclusion	45
5.1 Conclusion	45
5.2 Suggestion for future work	46
REFERENCES	47
Appendix A	50

LIST OF FIGURES

Fig. No.	Title	Page No.
1.	Schematic of Feed Forward Neural Network.	10
2.	Comparison of range and drift values obtained from six-degrees-of-freedom model with and without tip-off effect and fuzz factor, with corresponding range table values.	27
3.	Comparison of range and drift values obtained from six-degrees-of-freedom model with and without crosswind effect (Aerodynamic jump) on range and fuzz factor, with corresponding range table values.	29
4.	Comparison of range and drift values obtained from six-degrees-of-freedom model with and without range wind effect (Aerodynamic jump) on drift and fuzz factor, with corresponding range table values.	31
5	Schematic representation of FFNN for Model 1.	35
6.	Comparison of range table and model 1 predicted Range (R) and Drift (ψ) for varying ambient atmospheric conditions, and charge temperature.	37
7	Schematic representation of FFNN for Model 2.	38
8.	Comparison of range table and model 2 predicted elevation (θ) and Drift (ψ) for varying ambient atmospheric conditions, and charge temperature for given range.	40
9.	Comparison of range table and model 3 predicted standard range (X) at standard ambient atmospheric conditions.	43

LIST OF TABLES

Table No.	Title	Page No.
1.	Comparison of range and drift values obtained from six-degrees-of-freedom model with and without tip-off effect and fuzz factor, with corresponding range table values.	26
2.	Comparison of range and drift values obtained from six-degrees-of-freedom model with and without crosswind effect (Aerodynamic jump) on range and fuzz factor, with corresponding range table values.	28
3.	Comparison of range and drift values obtained from six-degrees-of-freedom model with and without range wind effect (Aerodynamic jump) on drift and fuzz factor, with corresponding range table values.	30
4.	Comparison of range and drift values obtained from trimmed six-degrees-of-freedom model for 5m/s range wind and cross wind separately.	32
5.	Comparison of range table and model 1 predicted Range (R) and Drift (ψ) for varying ambient atmospheric conditions, and charge temperature.	36
6.	Comparison of range table and model 2 predicted elevation (θ) and Drift (ψ) for varying ambient atmospheric conditions, and charge temperature for given range.	39
7.	Comparison of range table and model 3 predicted standard range (X) at standard ambient atmospheric conditions.	42

NOMENCLATURE

T	= Ballistic Air Temperature (ambient air temperature), °C
P	= Ballistic Air Pressure (ambient Air Pressure), mm Hg
Th	= Thrust
T _c	= Charge Temperature, °C
θ	= Firing Table Elevation, Firing angle, mils
ψ	= Bearing correction for Drift, mils
d	= Diameter of Rocket, mm
C _N , C _A	= Coefficient of normal and axial force
C _L , C _{D₀} , C _M	= Non-dimensional lift, drag, and pitching moment coefficients
C _X , C _Y , C _Z	= Coefficient longitudinal, lateral, vertical force
q̄	= Dynamic pressure, N/m ²
m	= mass, kg
u, v, w	= Velocity components in x, y and z body axes, m/s
V	= Air-relative speed, m/s
g	= Acceleration due to gravity, m/s ²
I _x , I _y	= Moment of inertia about x and y axis, kgm ²
I _{xy} , I _{xz} , I _{yz}	= Cross products of inertia, kgm ²
p	= Roll rate, rad/sec or deg/sec
q	= Pitch rate, rad/sec or deg/sec
r	= yaw rate, rad/sec or deg/sec
α	= angle of attack, rad or deg
β	= angle of side slip, rad or deg

R	= Range, m
θ	= Pitch attitude, mils
ϕ	= Roll attitude, rad or deg
ψ	= Heading angle, rad or sec
s	= Reference area, m^2
W_x, W_y, W_z	= Head/tailwind, crosswind, vertical wind components, m/s
δ	= Fin cant angle, rad or deg

Superscript

\cdot	= Derivative with respect to time
---------	-----------------------------------

Subscript

o	= Initial conditions
x,y,z	= component along x, y, and z direction
wind	= wind axes

Stability and control derivatives

$$\begin{aligned}
 C_{L\alpha} &= \partial C_L / \partial \alpha, & C_{Lq} &= \partial C_L / \partial (qd/2V), & C_{L\delta} &= \partial C_L / \partial \delta \\
 C_{m\alpha} &= \partial C_m / \partial \alpha, & C_{mq} &= \partial C_m / \partial (qd/2V) \\
 C_{lp} &= \partial C_l / \partial (pd/2V), & C_{l\delta} &= \partial C_l / \partial \delta \\
 C_{n\beta} &= \partial C_n / \partial \beta, & C_{nr} &= \partial C_n / \partial (rd/2V) \\
 C_{y\beta} &= \partial C_y / \partial \beta, & C_{yr} &= \partial C_y / \partial (rd/2V)
 \end{aligned}$$

CHAPTER 1

INTRODUCTION

Artillery forms an important wing of army to provide firepower during war as well as during cross boarder skirmishes with enemy. Artillery rocket systems are used in same manner as artillery gun systems to provide support to personnel in contact with the enemy in forward areas. A rocket system is made up of a number of sub-systems, each of which performs a function necessary to the successful performance of the system. In general, the artillery rocket system is composed of three main elements: a) the rocket, b) the launcher and c) the fire control device. Each of these in turn is composed of subsystems or components, each of which has a necessary function to permit successful operation¹.

An artillery rocket is composed of a payload of warhead and a propulsion motor to provide adequate acceleration. The rocket warhead has a shell of casing, which is hollow, and which may be aerodynamically shaped to serve as nose of the rocket¹. An appropriate high explosive is loaded into the casing. Actuation of explosive is performed by the fuze. In general the artillery rocket systems used by the several branches of the armed forces are classed as military systems. They are used to deliver some form of destructive warhead on enemy target. Artillery rockets may be used in almost unlimited number of ways. A ground-to-ground rocket is launched from a point on the ground to a target on the ground, whereas a ground to air rocket is launched from the ground against air borne target. Similarly air to air and air to ground rockets are launched from aircraft to engage target in air and ground respectively¹.

The effectiveness of artillery is largely judged by the accuracy in hitting the targets. Various error sources inherent in the rocket system, together with external conditions such as wind cause dispersion of payloads from its intended path. Error sources are labeled according to the phase of the flight. The flight path of the rocket is divided into three phases: 1) launch phase 2) boost phase and 3) the ballistic phase. Launch phase error includes the initial conditions transmitted to the rocket, by launcher and dynamic unbalance effect of the rocket. Boost phase errors result from the thrust malalignment, meteorological conditions, aerodynamic irregularities etc. Ballistic phase mainly includes error due to non-standard meteorological conditions. The accuracy of the rocket system depends upon the following major factors:

- 1) variation in initial launch conditions due to tip-off effect about the contact point, at the time of leaving the launcher.
- 2) aerodynamic jump due to wind at launch: The artillery rockets are generally ² given spin during launch to minimize the effect of thrust malalignment. Because of the spin , the rocket reacts gyroscopically to external wind just at the exit of launcher tube. This changes the orientation of the rocket causing substantial effect of crosswind on range and range wind on drift.
- 3) meteorological condition like, temperature, pressure, head/tail wind.
- 4) thrust malalignment during the boost phase of the trajectory.

The actual path traversed by the rockets are compared to predicted trajectory in order to calculate accuracy. The conventional models like (point mass, modified point mass, six-degrees-of-freedom models) predict all elements of trajectory from launch to

target. In these models it become essential that all the forces and moments affecting flight are to be accounted for in a well defined mathematical form².

However best of these models, have their limitations due to their inability to model all the problem variables adequately. For example, i) initial conditions at the time of rocket leaving the barrel (tip-off and aerodynamic jump) are not accounted for in any of the proposed model, ii) the models require aerodynamic coefficients as the input (e.g. drag coefficients, damping in roll derivative, lift curve slope etc) and the estimates available for these coefficients are not so reliable¹, and 3) the varying atmospheric conditions over the height traversed by the rocket are accounted for only in adhoc manner by using single weighted mean value of the variable like temperature, pressure, head/tail wind, cross wind².

It is thus realized that even the best mathematical models available to date are not reliable for the field applications because of accurate prediction are difficult for 1) the range obtainable for various firing angles, 2) the firing angle required for specific range. The obvious step is to improve the prediction capabilities by taking into account of the effects due to above mentioned problem variables. Thus suitable modification has to be incorporated into the present model to account for the above mentioned effects in the trajectory model.

The limitations of the mathematical model so far used for predicting the performance of the artillery rockets motivated us to look at an alternative approach to modelling. The feed forward neural network ^{3,4,5} provides one such potential way of modelling.

The neural network has been successfully used in diverse fields as signal processing, pattern recognition, system identification and control. In recent years, neural model of aircraft aerodynamics have been successfully developed for many applications relevant to aerospace engineering^{6,7,8}. For example neural modelling has been used for aircraft stability and control derivative of stable^{9,10,11}, unstable¹², aeroelastic aircraft¹³. It was envisaged that a neural model can be developed to replace the use of hitherto used mathematical model for solving the rocket related trajectory problems. Recently, the validity of the neural modelling had been demonstrated for three different applications relevant for artillery shell.¹⁴ For real life situations it was realized that the problem of trajectory, broadly speaking, could be divided into three categories under prevailing ambient atmospheric conditions 1) to predict range for chosen firing angle θ , 2) to predict required firing angle to achieve specified range, 3) to predict range that would have been achievable under standard atmospheric conditions. The next step is to identify the set of input-output variables for the network for each of the problems. Finally a suitable architecture for the neural network is to be searched to achieve acceptable functional mapping between input output variables for each of the problems

In the present work, all the above problems are addressed and adequately solved. For demonstrating the prediction capability of neural models developed, the data used is for the Grad-122mm Rocket, supplied by ARDE, Pune. Details of the data supplied, six-degrees-of-freedom model and various neural models are given in chapter 3. Details of the modelling for the three categories of the problems related to the rocket trajectory, along with result obtained for each of the three models are discussed in chapter 4. A brief overview of the neural network precedes these chapters 3 and 4 and is given in chapter 2.

The dissertation ends with chapter 5 containing conclusion and a few suggestions for the future work

CHAPTER 2

ARTIFICIAL NEURAL NETWORK

2.1 Introduction

A neural network is a parallel distributed processor that has a natural propensity for storing experimental knowledge and making it available for use. It resembles the brain in two respects, 1) knowledge is acquired by the network through learning process, 2) inter neuron connection strengths known as synaptic weights are used to store the knowledge. Neural networks are also referred to in the literature as neuro computers, connectionist networks, parallel distributed processors³, etc.

Artificial neural networks consist of group of neurons arranged in a layered structure. Each neuron receives signal from the neurons in the layer previous to itself and passes a signal on to the neuron in the following layer. The relationship between the summed inputs to a neuron and its output is governed by an ‘activation function’. Some of the commonly employed activation functions are the step function, the tangent-hyperbolic function, and the logistic (sigmoidal) function.

Out of these, the most often-used activation function is the sigmoidal function defined as

$$F(x) = \frac{1}{1 + e^{-\lambda x}}$$

Where λ is the logistic gain.

The sigmoidal function is continuous, monotonically increasing and continuously differentiable, and it asymptotically approaches fixed finite values as the input approaches infinity (+ or -).

Amongst the artificial neural networks, the feed forward neural networks (FFNNs) have found the favour with most researchers for application in aerospace engineering problems. The feed forward neural network consists of source nodes that constitute the input layer and one or more hidden layers and an output layer. Feed forward neural networks have neurons arranged in layers like directed graphs, implying a unidirectional flow of signals, and thus are static in nature. This kind of modeling develops input-output relationship of a black box kind. Each of the connection between neurons is assigned its individual weight and it is adjusted so as to yield the required output corresponding to the known set of inputs. An assignment of weights is done during the training sessions of the network.

2.2 Back Propagation Algorithm

One of the efficient methods for training the FFNN is the back propagation algorithm (BPA)³. Back propagation algorithm consists of a forward and backward pass through different layers of the network. During the forward pass, the input vector is applied to the input nodes of the network and its effect propagates through the network layer by layer. The connective weights are all kept fixed during the forward pass. On the other hand, in the backward pass, the weights are updated in accordance with error correction rule. Specifically, the actual response of the network is subtracted from the desired response to produce an error signal. This error signal is then propagated

backward against the direction of the connective weights. There are the four steps for back propagation algorithm.

- a) Initialization: Start with a reasonable network configuration and set all the synaptic weights randomly.
- b) Forward Computation: Let a training example represented by $x(n)$ be applied to the input nodes. Then the output of the network is computed by proceeding through the network, layer by layer. Next, the error signal is computed using difference between the desired response vector and the output vector.
- c) Backward Computation: The back propagation algorithm is based on optimizing a suitably defined error function. At each point, the local output error cost function defined by the sum of the squared error is computed. The weights of the network are adjusted in such a way that the mean squared error (MSE) is minimized.

The MSE is given by

$$MSE = \frac{1}{mn} \sum_{i=1}^m \sum_{j=1}^n [Y_i(j) - X_i(j)]^2$$

where Y and X are the desired and predicted outputs, n is the number of data points and m is the number of output variables.

- d) Step (b) to (c) are repeated for each training pair in the training set until the error for the entire set is less than the prescribed value or the number of iterations exceed the prescribed limit.

The training algorithm is recursive in nature and it needs repetitive training sessions to achieve the required learning. There are many network influence (tuning) parameters like the learning rate, the momentum rate, the number of hidden layers, the number of iterations, the logistic gain, etc., that affect the accuracy of functional mapping

between the input and the output variables. There are no set rules for fixing values of these influence parameters. In literature, a few guidelines are available to guide the choice of these parameters. However, the final choice of fine tuning of these parameters is to be achieved by trial and error for the given problem, and it is a crucial step in finding a suitable neural model for the problem. Some of the guidelines and thumb rules for training of neural network are given in Appendix A.

The neural network model is first trained on the known sets of input-output pairs of experimental or recorded data. The trained network is then capable of predicting the required output based on known (measured) input variables. This approach does not require a mathematical model or a transfer function relating the input-output data but only a sufficient set of input-output pairs of data. The choice of inputs that are likely to affect the output to be predicted by the neural model is of critical importance. The selection of inputs for the given problem is based on the understanding of the physics of the problem and engineering judgment.

In the present work, a neural model is proposed for the trajectory modeling of an artillery rocket fired from a launcher. A non-linear relationship is mapped by the neural network between the input variables such as ranges, wind velocity, ballistic air temperature, ballistic air pressure and charge temperature with the output variables such drift (Ψ) and angle of firing (θ). A schematic of such a neural model is shown in Fig. 1. For a typical neural model used in the present work, the choice of the input and output variables for mapping projectile dynamics is dictated by the physical understanding of the phenomenon governing the rocket dynamics. Once the input and output variables for the

feed forward artificial network (FFNN) are selected, the FFNN model of rocket dynamics is achieved without the need of a formal model structure formulation.

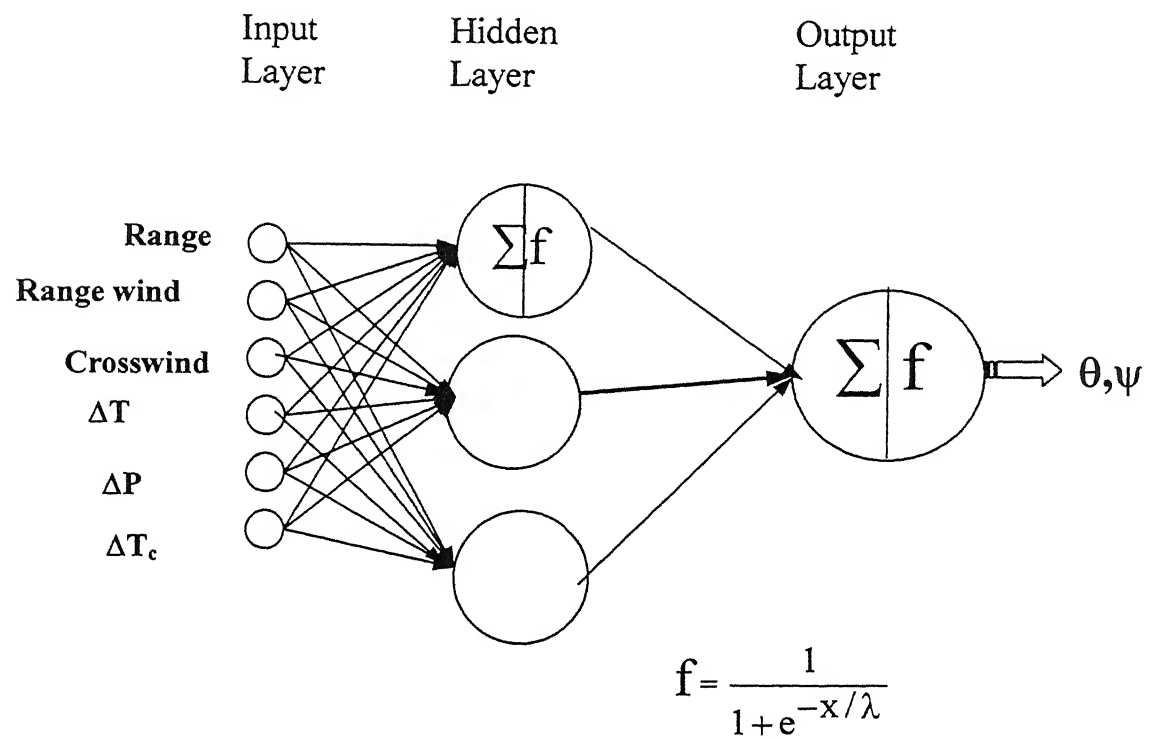


Fig. 1 Schematic of feed forward neural network.

CHAPTER 3

TRAJECTORY AND RANGE MODELLING OF ARTILLERY ROCKET

3.1 General

Artillery rockets are class of projectiles, which still continue to be of interest and further investigation for many new ballisticians and user agencies. In present work, we are specifically to focus on flight of fin stabilized, dynamically stable, unguided artillery rockets.

Presently, the conventional approach to modeling of trajectory and range of artillery rockets has been by postulating a suitable mathematical model consisting of equations of motion. There are numerous such forms of trajectory model involving different basic assumptions and having different complexities of solution. We shall briefly outline two of them in subsequent sections.

3.2 The Point mass model

In this model it is assumed that only aerodynamic force acting on the projectile is drag. It provides fairly accurate estimate of range during unpowered phase, for an adequately stable projectile. However, this model doesn't account for the effect of spin, lift, side force, pitching and yawing moment of the projectile and thus fails to predict accurately, the effect of wind on range and drift during boost (powered) phase. To estimate first order wind effects point mass equations of projectile motion may be expressed as follows:

The equations of motion along and perpendicular to the trajectory are given by

$$m \frac{dV}{dt} = Th - D - mg \sin \theta \quad (3.2a)$$

$$\frac{d\theta}{dt} = -\frac{g \cos \theta}{V} \quad (\text{trajectory turn over rate}) \quad (3.2b)$$

and the distance along x and y are computed using

$$\frac{dx}{dt} = V \cos \theta \quad (3.2c)$$

$$\frac{dy}{dt} = V \sin \theta \quad (3.2d)$$

where x denotes the range, y the height and D the Drag..

3.3 Six-degrees-of-freedom model:

The requirements for a trajectory program needed for predicting flight variables are: 1) that the trajectory be three-dimensional, 2) that provision be made for arbitrary wind velocity, azimuth and other meteorological conditions and 3) that nonlinear aerodynamics with respect to flow incidence angle (angle of attack) be included. The first two requirements are obvious since, in the consideration of side winds, the trajectory is three-dimensional and the wind velocity, azimuth and meteorological conditions (temperature, pressure) are arbitrary. The third requirement is imposed because the introduction of surface winds during launch can create large angle of attack, which greatly exceeds the linear range of aerodynamic coefficients.

A trajectory simulation incorporating the above requirements is presented below.

In addition to the above requirements, this simulation assumes a vehicle with six degrees-

of-freedom and aerodynamic symmetry in roll. The six-degrees-of-freedom model equations are given below¹⁵.

$$\dot{u} = (\bar{q} s/m) C_x - qw + rv - g \sin \theta + Th/m \quad (3.3a)$$

$$\dot{v} = (\bar{q} s/m) C_y - ru + pw + g \sin \phi \cos \theta \quad (3.3b)$$

$$\dot{w} = (\bar{q} s/m) C_z - pv + qu + g \cos \phi \cos \theta \quad (3.3c)$$

$$\dot{p} = \bar{q} sbC_l + qr(I_y - I_z) / I_x \quad (3.4a)$$

$$\dot{q} = \bar{q} sbC_m + rp(I_z - I_x) / I_y \quad (3.4b)$$

$$\dot{r} = \bar{q} sbC_n + pq(I_x - I_y) / I_z \quad (3.4c)$$

$$\dot{\phi} = p + q \tan \theta \sin \phi + r \tan \theta \cos \phi \quad (3.5a)$$

$$\dot{\theta} = q \cos \phi - r \sin \phi \quad (3.5b)$$

$$\dot{\psi} = r \cos \phi \sec \theta + q \sin \phi \sec \theta \quad (3.5c)$$

To drive the spatial position equations, above equation were used to transform the body-axis velocity (u, v, w) into earth-fixed-axis. The equations are:

$$\begin{aligned} \dot{X} &= u \cos \psi \cos \theta + v(\cos \psi \sin \theta \sin \phi - \sin \psi \cos \phi) \\ &\quad + w(\cos \psi \sin \theta \cos \phi + \sin \psi \sin \phi) \end{aligned} \quad (3.6a)$$

$$\begin{aligned} \dot{Y} &= u(\sin \psi \cos \theta) + v(\sin \psi \sin \theta \sin \phi + \cos \psi \cos \phi) \\ &\quad + w(\sin \psi \sin \theta \cos \phi - \cos \psi \sin \phi) \end{aligned} \quad (3.6b)$$

$$\dot{Z} = u \sin \theta - v \cos \theta \sin \phi - w \cos \theta \cos \phi \quad (3.6c)$$

Aerodynamic model used in this analysis is as given below:

$$Cx = -C_{Dwind} \cos \alpha \cos \beta + C_L \sin \alpha - Cy_{wind} \cos \alpha \sin \beta \quad (3.7a)$$

$$Cy = Cy_{wind} \cos \beta - C_{Dwind} \sin \beta \quad (3.7b)$$

$$C_z = -C_L \cos \alpha - C_{D_{wind}} \sin \alpha \cos \beta - C_{y_{wind}} \sin \alpha \sin \beta \quad (3.7c)$$

where

$$C_L = C_{L_0} + C_{L\alpha}\alpha + C_{Lq}(qd/2v) \quad (3.8a)$$

$$C_{y_{wind}} = C_{y\beta}\beta + C_{yr}(rd/2v) + C_{yo} \quad (3.8b)$$

$$C_{D_{wind}} = Cd \quad (3.8c)$$

$$C_l = C_{lp}(pd/2v) + C_{l\delta}\delta \quad (3.9a)$$

$$C_m = C_{m_0} + C_{m\alpha}\alpha + C_{mq}(qd/2v) \quad (3.9b)$$

$$C_n = C_{n_0} + C_{n\beta}\beta + C_{nr}(rd/2v) \quad (3.9c)$$

wind model used in this analysis is as given below :

$$u' = u - W_x \cos \theta \cos \psi - W_y \cos \theta \sin \psi + W_z \sin \theta \quad (3.10a)$$

$$\begin{aligned} v' &= v - W_x (\cos \psi \sin \theta \sin \phi - \sin \psi \cos \phi) \\ &\quad - W_y (\cos \psi \cos \phi + \sin \psi \sin \theta \sin \phi) \\ &\quad - W_z (\cos \theta \sin \phi); \end{aligned} \quad (3.10b)$$

$$\begin{aligned} w' &= w - W_x (\cos \psi \sin \theta \cos \phi + \sin \psi \sin \phi) \\ &\quad - W_y (\sin \psi \sin \theta \cos \phi - \cos \psi \sin \phi) \\ &\quad - W_z \cos \theta \cos \phi; \end{aligned} \quad (3.10c)$$

$$V = \sqrt{u'^2 + v'^2 + w'^2} \quad (3.11)$$

$$\text{Thus } \alpha = \tan(w'/u') \text{ and } \beta = \tan(v'/u')$$

where W_x , W_y , W_z are the wind component blowing toward the north and east.

However, the indeterminability of many of the initial conditions and aerodynamic coefficients which are required as input, results in model not giving desired results. Even if accurate aerodynamic coefficients are available, there are several other uncertainties,

especially for tube launched artillery rocket, that would affect range estimates. A few such uncertainties associated with tube launched artillery rocket are outlined below:

- 1) Tip-off effect²
- 2) Effect of wind at launch² – Aerodynamic jump

Tip-off-effect

During the release of the rocket from the launch tube, the rocket tends to rotate about the rear end (at the exit of launcher) under the action of gravity and other applied forces. The angle of elevation deviation due to this can be approximated by the following expression²

$$\Delta\theta = -\frac{(L - X_{cg}) \times g \times \cos\theta}{V^2} \quad (3.12)$$

where:

L is Rocket length, X_{cg} is cg position from nose

g is acceleration due to gravity, θ is firing elevation

Effect of wind at launch -Aerodynamic Jump:

The artillery rockets are generally given spin during launch to minimize the effect of thrust malalignment. Because of this spin, the rocket reacts gyroscopically to external wind at exit. This changes the angular orientation of the rocket causing substantial effect due to cross wind on range and range wind on drift.

For spun projectiles crosswind will also have an effect in the vertical plane due to the time taken to adapt to the air-relative zero yaw position. This occurs whenever projectile emerges into a region of significantly different wind-relative zero yaw attitude, but most commonly has its effect on a projectile exiting from the launcher. This effect is linear in the range and is dependent on the wind at one point. It is thus termed as

aerodynamic jump effect. It is shown in Ref. 2 that change in elevation due to a crosswind can be approximated by

$$\frac{pI_x C_{L\alpha} W_y}{mdV^2 C_{M\alpha}} \quad (3.13a)$$

(Upwards for a crosswind from the right)

Effect of range wind on drift is similar to above mentioned effect. There is similar term due to the transverse component of a head wind. The head wind affects drift performance of rocket. The total effect is called windage jump. It is shown in Ref. 2, that the change in drift (rad) due to range wind for a projectile can be approximated by:

$$\frac{pI_x C_{L\alpha} W_x}{mdV^2 C_{M\alpha}} \quad (3.13b)$$

(Right for a crosswind from the behind)

From the application point of view, the six-degrees-of-freedom model has been used to predict range and drift for different elevations and compared with range table data. Study has been carried out to predict

- 1) range and drift for various elevations under standard atmosphere,
- 2) range and drift in presence of head, tail, cross winds.

The result and discussion of this study has been discussed in the next chapter.

3.4 Range Tables-fired data.

Due to non-availability of raw fired data, the range table for the Grad-122mm Russian rocket (hereafter Grad rocket for convenience) was used for the present study. Generally, range table is prepared by trimming assumed trajectory model using raw fired data and known meteorological conditions. Since as stated earlier, trajectory model

suffers from its well known limitations, therefore a large number of fuzz factors are required to be introduced in the model. Moreover such fuzz factors are finalized, after carrying out exhaustive validation firing under different meteorological conditions. Many a times, the use of such factors no way appears to be consistent with the physics of the problem. Thus, although it may be useful to prepare range table, but may not be quite accurate to predict performance of rocket when fired under widely varied meteorological conditions.

The range table lists range obtainable for various firing elevations (hereafter referred to as firing angels θ , under standard calm atmospheric conditions, also time of flight and correction to bearing drift is provided. The correction to these listed values of range for each value of θ due to following variations at the time of firing are also provided.

- 1) Variation in ambient atmospheric conditions (temperature, pressure)
- 2) Head/tail wind
- 3) Cross wind.
- 4) Charge Temperature

3.5 The Neural Models.

The limitations of mathematical models so far used for predicting range of artillery rockets motivated to look at an alternative approach to modelling. The feed forward neural network provides one such potential way of modeling. The neural model needs identifications of suitable input output variables to map the relationships existing between them. The functional relation is obtained by training with measured input-output

variables and then the trained network is used to predict the output for set of inputs not seen by network during the training phase. The data from the range table provided by ARDE Pune for Grad rocket is used for the present work.

For the purpose of developing a neural model, the data from the range table was randomly selected to form sets having chosen number of data points, say, 95 or 48 or 30 or 15. One of these sets is used for training the network then two sets of data points each, are taken for validation set, which are different from the training set. As mentioned in appendix A the acceptability of the network architecture is decided by comparing the MSE during the training phase and validation phase. The thumb rule applied is that MSE for the two validation sets should not be greater than about two to three times the MSE for the training set. Of course, the MSE permitted on the training set is prescribed and kept below it, while choosing the architecture of network, i.e. while choosing the learning rate, the momentum rate, the number of iterations, the number of neurons, etc.

Finally, one set of data, not used for the above two stages of training or validation is used to predict required output. This output is compared with known output corresponding to the same inputs, and thus shows acceptability of neural model in predicting the required output variable.

From application point of view the following three types of modelling problems were taken up for study. The neural network models for these three cases are presented in details in next chapter along with results obtained via each of these models. However, a brief outline of all the three models follows.

Model 1

This model deals with direct problem of modelling range and drift experienced by Grad-rocket. These output variables of neural model would depend on firing angle θ , air temperature and pressure, head /tail wind, cross wind and charge temperature .

Model 2

This Model deals with the inverse problem of predicting firing angle θ , required to achieve desired range, given the air temperature and pressure, head/tail wind, cross wind and charge temperature. It also predicts drift. This is what a user would require to know in most of the real life applications.

Model 3

This Model was developed to predict range that would be obtainable under standard conditions, given the measured data of range obtained under varying atmospheric conditions like air temperature and pressure, head/tail wind, cross wind and charge-temperature. Such a prediction capability would be useful to compare performance of different rockets under identical (standard) conditions. It is not practical to obtain data for different rocket or for same racket on different days under similar conditions, and thus compare the relative performance. If data collected under different ambient conditions can be used for training the network, and then be able to predict range that would result under chosen standard ambient condition, one could then compare results for the different rockets or the rocket fired at different times or days.

The result and discussion for all the above three Models, along with details of modelling are presented in next chapter.

CHAPTER 4

SIX-DEGREES-OF-FREEDOM MODEL, NEURAL MODELS, RESULTS AND DISCUSSION

In this chapter, we first analyze the data of Grad rocket, supplied by ARDE, Pune.

Next, the difficulties faced by six-degrees-of-freedom trajectory model, to predict rocket trajectory are discussed. Finally, details of all the three neural models along with the results are discussed.

4.1 Analysis of Grad-Rocket data:

The range/drift data used in present study was supplied in the form of table. The table lists range obtainable for various firing elevations (firing angle θ) under standard and calm atmospheric conditions. Also time of flight and correction for bearing is provided. The correction to these listed values firing angles due to following variations at the time of firing are also provided:

- 1) Variations in ambient atmospheric conditions (temperature, Pressure)
- 2) Head/tail wind in Powered and un powered phase
- 3) Crosswind
- 4) Charge Temperature

These firing angles listed in the firing data table vary from 84 mils to 811mils. These firing angles corresponds to variation from 4.725° to 45.61875° .

The table has following columns

- 1) Standard Range
- 2) Elevation

- 3) Range correction for 1 mil change in elevation
- 4) Deflection correction for 10m/s cross wind in powered flight phase
- 5) Deflection correction for 10m/s range wind in powered flight phase
- 6) Elevation correction for 10m/s range wind in powered flight phase
- 7) Elevation correction for 10m/s cross wind in powered flight phase
- 8) Deflection correction for 10m/s cross wind in unpowered flight phase
- 9) Range correction for 10m/s range wind in unpowered flight phase
- 10) Range correction for 10°C Change in air temperature
- 11) Range correction for 10 mm of Hg change in air ground pressure
- 12) Range correction for 10° C change in charge temperature(negative change)
- 13) Range correction for 10° C change in charge temperature(positive change)

Nonstandard range calculation:

The Data table was used to prepare input output data sets for the neural model.

The Range R for nonstandard condition was calculated as follows:

$$R = X - [C_1(W_x)Y + C_2(W_y)Y + C_3(W_x) + C_4(\Delta T) + C_5(\Delta P) + C_6(\Delta T_c)]$$

Where X = range at standard condition for a particular firing elevation.

C_1 = elevation correction for 10m/s range wind in Powered flight phase .

Y = change in range for 1 mil change in elevation.

W_x =weighted mean value of head/tail wind .

W_y =weighted mean value of cross wind.

C_2 = elevation correction for 10m/s crosswind in powered flight phase.

C_3 = range correction for 10 m/s range wind in unpowered flight phase.

C_4 = range correction for 10°C change in air temperature.

ΔT = change in temperature from standard atmosphere ($^{\circ}\text{C}$).

C_5 = range correction for 10mm of Hg change in ground air pressure.

ΔP = change in ground air pressure from standard atmosphere(mm of Hg).

C_6 = range correction for 10° change in charge temperature.

ΔT_c = change in charge temperature.

It is noted that range is affected not only by range wind but by crosswind also in powered phase of rocket trajectory. In same way drift is also affected by range and cross wind both in powered phase of flight.

To illustrate the calculation of range R for nonstandard conditions, consider the firing elevation of 217 mils. The data table gives standard range 10,000 m

.Let us assume range wind is 7 m/s, crosswind is 5m/s , change in air temperature is 6°C , change in air pressure is 5 mm and change in charge temperature is 8°C .

For firing angle 217 mils from table we have

$$C_1 = 11.1 \text{ mils/ 10m/s}$$

$$C_2 = 13.2 \text{ mils/ 10m/s}$$

$$Y = 41 \text{ m/mil}$$

$$C_3 = 78 \text{ m/ 10m/s}$$

$$C_4 = 87 \text{ m/10}^{\circ}\text{C}$$

$$C_5 = 60 \text{ m/10mm of Hg}$$

$$C_6 = 167 \text{ m/10}^{\circ}\text{C}$$

$$R = 10000 - [(-1.11 \times 7 \times 41) + (-1.32 \times 5 \times 41) + (-7.8 \times 7) + (-8.7 \times 6) + (6.0 \times 5) + (-16.7 \times 8)]$$

$$= 10800 \text{ m}$$

Bearing correction = deflection correction for range wind in powered flight phase
+ deflection correction for cross wind in powered flight phase
+ deflection correction for cross wind in unpowered flight phase

$$\psi = -[(-0.3 \times 7) + (5.2 \times 5) + (-0.5 \times 5)] = -21.4 \text{ mils}$$

Implication of the deflection correction is that the rocket would drift to left (looking from behind in the direction of firing) by angle ψ . To hit the target, the rocket is fired by aiming to the right by angle ψ . This would in turn ensure that the target is hit after the drift that the rocket would experience due to wind.

Following the above procedure, the data given in the table form was converted into a convenient form for its use in neural models to be developed.

Specifically the data yielded the sets of data, each set having standard range X, Non-standard range R, deflection angle ψ , ambient temperature and pressure, crosswind, head/tail wind and charge-temperature for corresponding firing angle θ .

4.2 Modelling of rocket trajectory using six degree trajectory model

As discussed earlier, six degree-of-freedom trajectory model is used to predict

- 1) range and drift of artillery rocket when fired under standard atmosphere (no wind conditions).
- 2) range and drift of artillery rocket when fired under non-standard condition (wind is present). It was also mentioned that the indeterminability of many of initial conditions and aerodynamic coefficients which are required as inputs, results in model not giving desired results. In order to reduce the uncertainties with the aerodynamic coefficients, the wind tunnel estimates of Grad-rocket configuration¹⁶ were used in the

trajectory model. The geometric, mass, moment and thrust characteristics of grad-rocket were supplied by ARDE, Pune.

Trajectory model was run with wind tunnel estimates of aerodynamic coefficients of Grad-rocket to predict range and drift for various elevations. The atmosphere assumed for this case was standard atmosphere. Initially, the tip-off effects was not modeled. It could be seen from Table 1 that the predicted ranges at lower elevations did not match with the range table values. To improve the matching, approximate expressions for tip-off was introduced into the model and the trajectory program was re-run for all these elevations. Table 1, Column 4 presents these modified values of ranges after the introduction of tip-off effect in the trajectory model. It could be seen that there was appreciable improvement in prediction as far as ranges in all elevations are concerned. However, the drift values were still very much off as compared to the range table value. The differences between the predicted ranges/drifts and range table values were primarily due to inaccurate modelling of tip-off effect using approximate expression². In order to improve matching, a trim factor (fuzz factor) was used to enhance the contribution of tip-off to range and drift. Column 5 of Table 1(a) and 1(b) present the values of predicted range and drift using fuzz factor respectively. Figure 2 summarizes the improvements in range and drift at different elevations with the introduction of tip-off effect and fuzz factor respectively.

Next exercise undertaken was to model the effect of range wind and crosswind on range and drift of rocket at different elevations. It may be mentioned that the effect of range wind and crosswind on the trajectory of rocket is widely different for powered and unpowered phase. During powered phase, range wind and crosswind affect both range

and drift, however in unpowered phase range wind affects range and crosswind affects drift only. The trajectory model with tip-off effect included was run to predict the effect of wind in range and drift. To start with, the phenomena of aerodynamic jump as initial condition was not modeled and range and drift were predicted at different elevation using the trajectory model. The trajectory model was run assuming non-standard atmosphere having crosswind of magnitude 10m/s. Column 3 of Table 2 shows the values of predicted range and drift for different elevations. Column 2 shows the range table values. Comparing Column 2 and 3 of Table 2(a) and then Table 2(b), it was observed that range and drift at lower elevations did not match satisfactorily. Next step was to model the initial condition due to aerodynamic jump effect. The approximate expression representing the correction in range due to aerodynamic jump (due to crosswind) with and without fuzz factor were introduced in the trajectory model. Referring Table 2, it can be observed that the introduction of approximate expression for aerodynamic jump did not yield better results. However, using a ‘trim factor’ or fuzz factor of 20 in the expression of aerodynamic jump, the response of the rocket to crosswind improved appreciably. Further, it can be seen that, the introduction of fuzz factor, no way helped in improving drift values. Infact, the drift prediction at lower elevations got deteriorated.

Figure 2 summarizes the observation made referring the Table 2.

In order to model the effect of range wind on range and drift, trajectory model was run again with and without modelling the aerodynamic jump effect. The atmosphere here again was also assumed non-standard having range wind of magnitude 10m/s. Referring Table 3(a) for range, it could be stated that the modelling of aerodynamic jump, did not yield any improvement in the drift prediction, however, with the use of fuzz

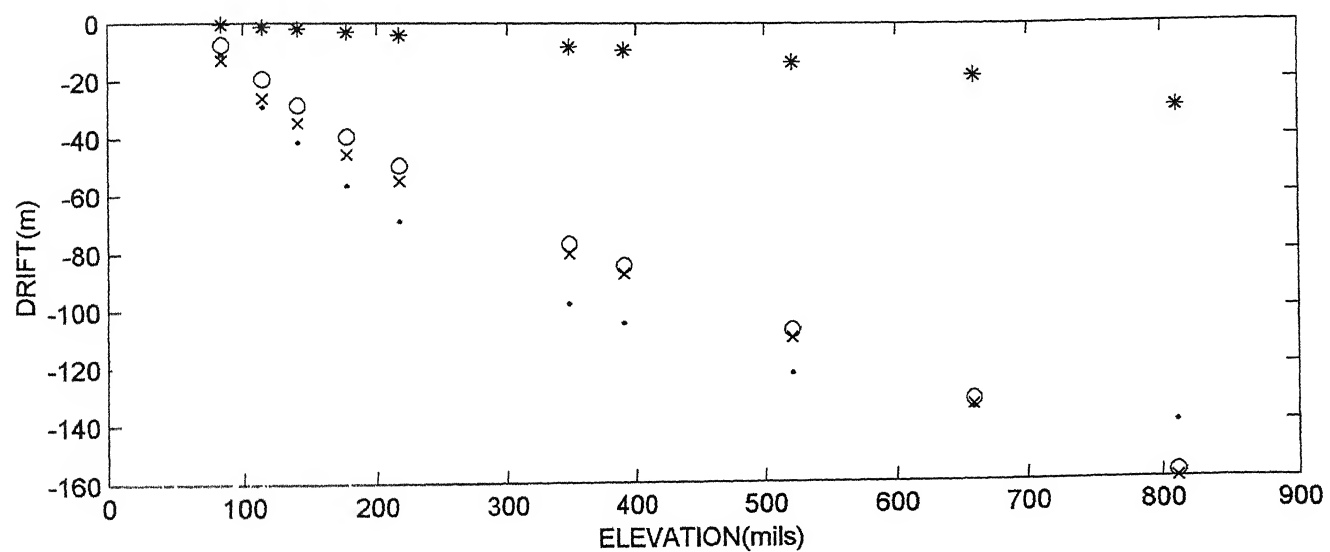
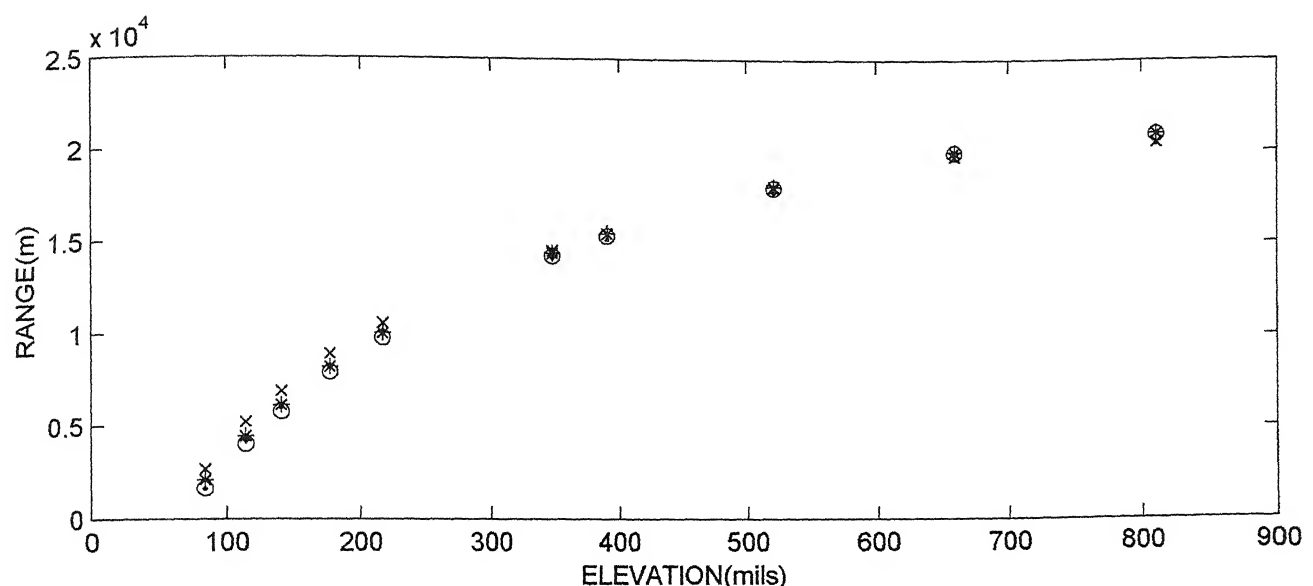
Table 1. Comparison of range and drift values obtained from six-degrees-of-freedom model with and without Tip-off effect and fuzz factor, with corresponding range table values.

Table (2a)

ELEVATION (mils)	RANGE (m)			
	RANGE TABLE	SIXDEGREES	SIXDEGREES WITH TIP-OFF- EFFECT	SIXDEGREES WITH TIP-OFF- EFFECT AND FUZZ FACTOR
84	1600	2692.07	2094.2	1635.6
114	4200	5247.1	4432.6	4030.8
140	6000	6924.5	6155.9	5812.1
177	8200	8956.0	8216.1	7934.81
217	10000	10612.7	10061	9828.9
348	14200	14557.9	14424.5	14284.5
390	15200	15507.8	15481.7	15359.2
521	17800	18027.6	18102.2	18020.5
659	19600	19730	19967.5	19920.6
811	20400	20486.1	20962.6	20927.2

Table (2b)

ELEVATION (mils)	DRIFT (m)			
	RANGE TABLE	SIXDEGREES	SIXDEGREES WITH TIP-OFF- EFFECT	SIXDEGREES WITH TIP-OFF- EFFECT AND FUZZ FACTOR
84	-10.99	-13.04	-0.59	-7.62
114	-28.86	-25.95	-1.412	-19.43
140	-41.23	-34.65	-2.129	-28.40
177	-56.34	-45.49	-3.161	-39.39
217	-68.71	-54.80	-4.30	-49.62
348	-97.57	-80.07	-8.22	-76.77
390	-104.4	-87.21	-9.51	-84.37
521	-122.3	-109.9	-13.67	-107.2
659	-134.6	-133.6	-18.23	-131.42
811	-140.2	-159.92	-29.48	-157.64



- RANGE TABLE
- × SIXDEGREE
- * SIX DEGREE WITH TIP-OFF EFFECT
- SIX DEGREE WITH TIP-OFF EFFECT AND FUZZ FACTOR

Fig 2. Comparison of range and drift values obtained from six-degree-of-freedom model with and without tip-off effect and fuzz factor, with corresponding range table values.

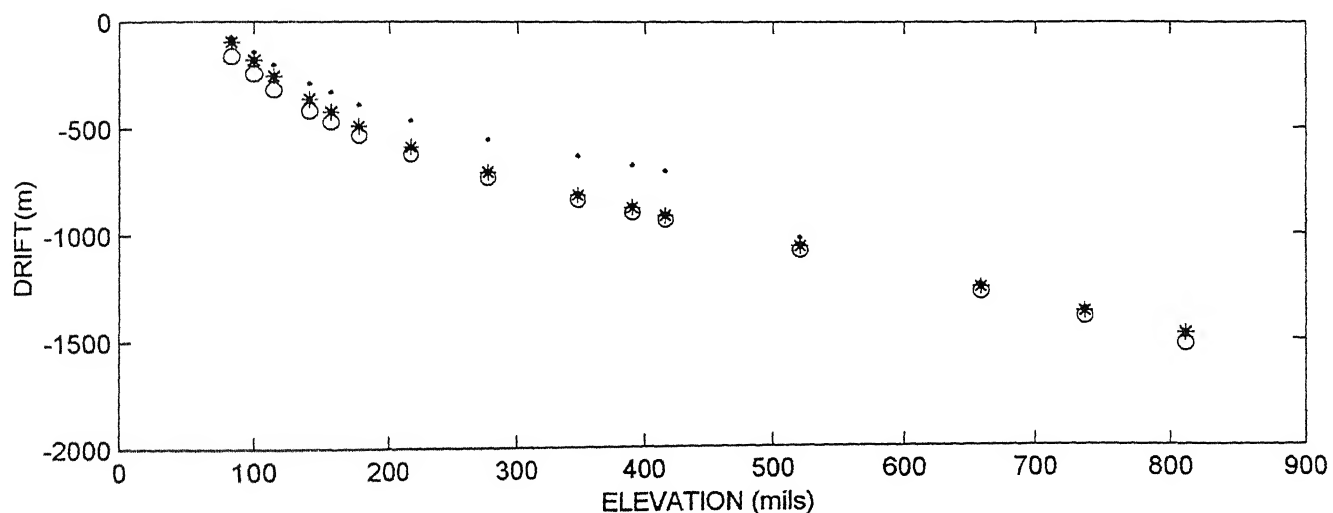
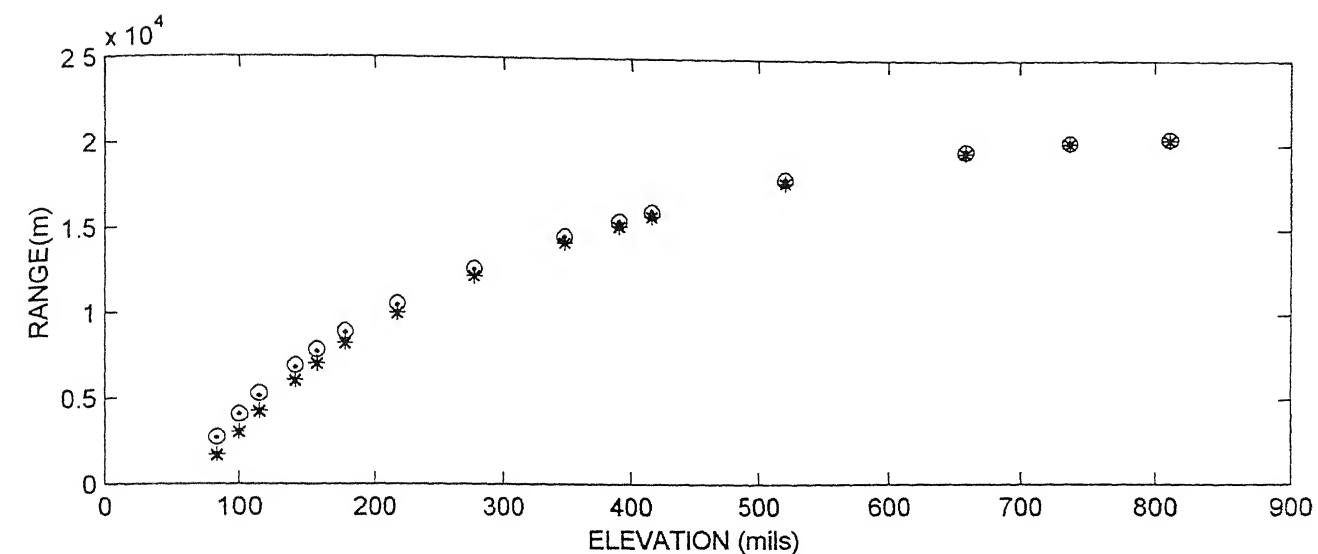
Table 2. Comparison of range and drift values obtained from six-degree-of-freedom model with and without crosswind effect (10m/s) (Aerodynamic jump) on range and fuzz factor, with corresponding range table values.

Table(2a)

ELEVATION (mils)	RANGE TABLE	RANGE (m)		
		SIXDEGREE	SIXDEGREE WITH CROSSWIND EFFECT ON RANGE	SIXDEGREE WITH CROSSWIND EFFECT ON RANGE AND FUZZ FACTOR
84	2698	1634.6	1691	2752.8
114	4075	2983.9	3041.1	4090.6
140	6832	6025.4	6073.7	6957.6
177	8873.2	8208.7	8248	8973.2
217	10541	9999.2	10031	10617
348	14535	14168	14187	14538
390	15508	15156	15173	15483
521	18018	17756	17768	17986
659	19732	19526	19533	19666
811	20400	20324	20329	20387

Table(2b)

ELEVATION (mils)	RANGE TABLE	DRIFT (m)		
		SIXDEGREE	SIXDEGREE WITH CROSSWIND EFFECT ON RANGE	SIXDEGREE WITH CROSSSWIND EFFECT ON RANGE AND FUZZ FACTOR
84	-73	-93.557	-97.026	-161.64
114	-202.18	-251.65	-255.13	-318.08
140	-288.84	-360.11	-362.96	-415.02
177	-386.64	-486.22	-488.48	-530.05
217	-461.72	-584.64	-586.42	-619.18
348	-627.7	-812.32	-813.42	-834.1
390	-671.9	-870.79	-871.83	-891.26
521	-1014.6	-1055.8	-1056.8	-1075.7
659	-1233	-1250	-1251.1	-1271.7
811	-1484.5	-1469.3	-1471.7	-1518.3



- | | |
|---|---|
| • | RANGE TABLE |
| × | SIXDEGREE |
| * | SIXDEGREE WITH CROSSWIND EFFECT ON RANGE |
| ○ | SIX-DEGREE WITH CROSSWIND EFFECT ON RANGE AND FUZZ FACTOR |

Fig.3 Comparison of range and drift values obtained from six-degree-of-freedom model with and without crosswind effect (Aerodynamic jump) on range and fuzz factor, with corresponding range table values.

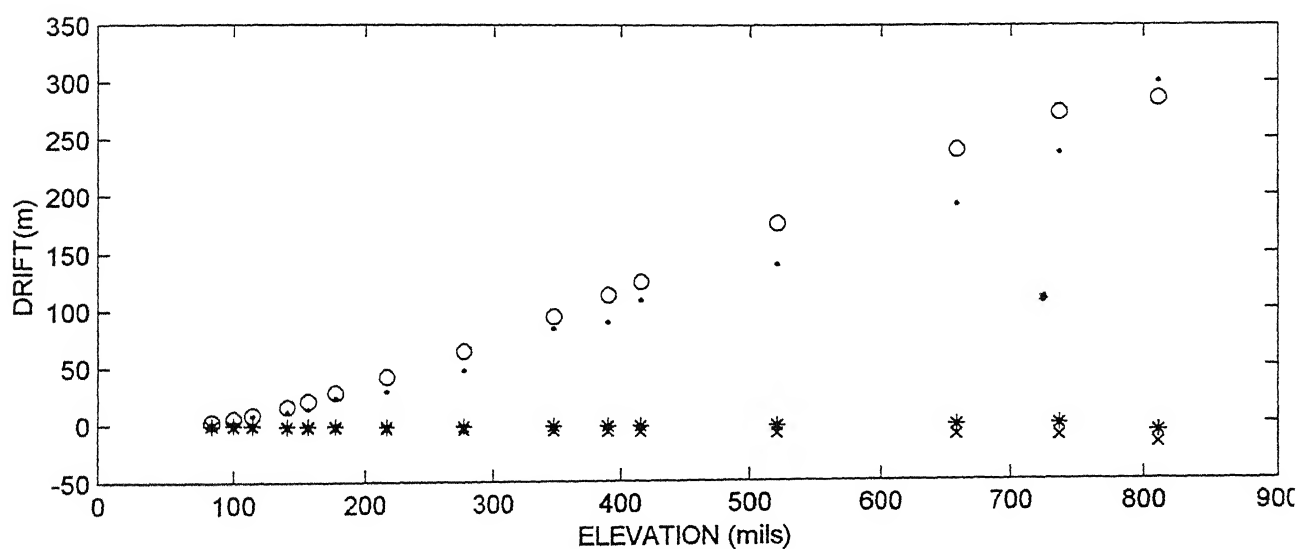
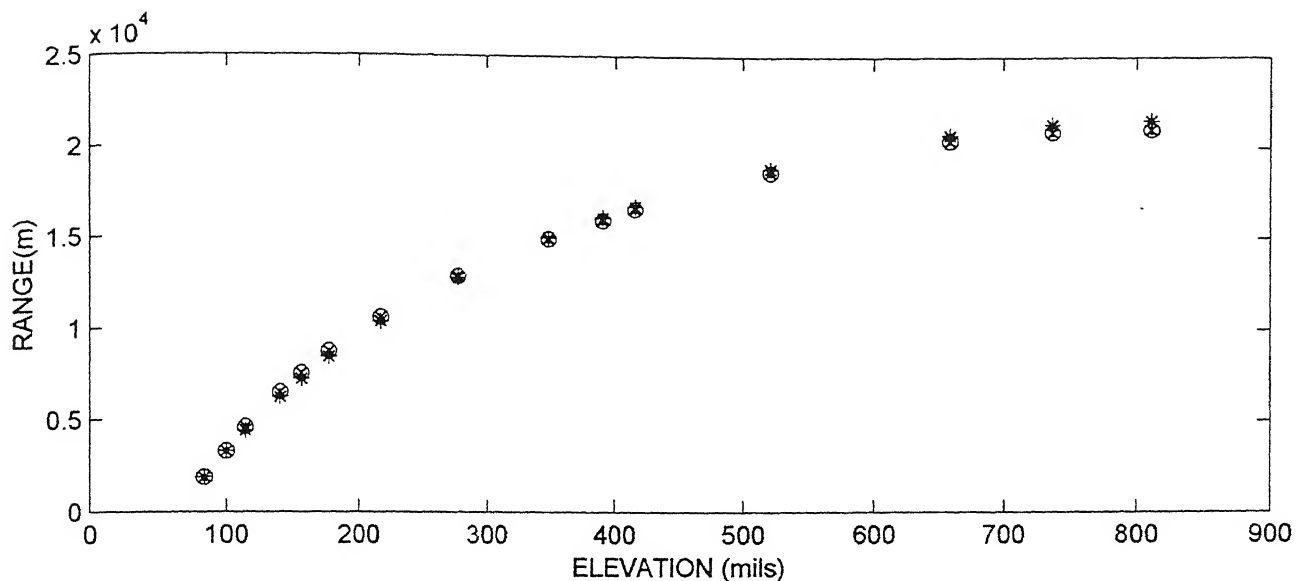
Table 3. Comparison of range and drift values obtained from six-degrees-of-freedom model with and without range wind (10m/s) effect (Aerodynamic jump) on drift and fuzz factor, with corresponding range table values.

Table(3a)

ELEVATION (mils)	RANGE (m)			
	RANGE TABLE	SIXDEGREE	SIXDEGREE WITH RANGE WIND EFFECT ON DRIFT	SIXDEGREE WITH RANGE WIND EFFECT ON DRIFT AND FUZZ FACTOR
84	1799	1880.2	1880.2	1880.1
114	4541.1	4614.5	4614.5	4614.0
140	6413.4	6519	6519	6519
177	8691.7	8787.3	8787.3	8787.2
217	10533	12899	12899	12899
348	14852	14950	14950	14950
390	15899	15975	15975	15975
521	18570	18658	18658	18657
659	20345	20408	20408	20407
811	20897	21021	21021	21019

Table(3b)

ELEVATION (mils)	DRIFT (m)			
	RANGE TABLE	SIXDEGREE	SIXDEGREE WITH RANGE WIND EFFECT ON DRIFT	SIXDEGREE WITH RANGE WIND EFFECT ON DRIFT AND FUZZ FACTOR
84	1.5707	-0.387	-0.273	2.688
114	8.246	-1.039	-0.658	9.24
140	11.78	-1.563	-0.902	16.277
177	24.149	-2.28	-1.154	28.117
217	29.45	-3.00	-1.331	42.064
348	83.64	-5.294	-1.608	94.231
390	89.53	-5.986	-1.582	112.9
521	139.79	-8.095	-1.294	175.54
659	192.41	-9.988	-0.715	240.36
811	300.4	-17.86	-6.634	285.24



- RANGE TABLE
- × SIXDEGREE
- * SIXDEGREE WITH RANGEWIND EFFECT ON DRIFT
- SIX-DEGREE WITH RANGEWIND EFFECT ON DRIFT AND FUZZ FACTOR

Fig 4. Comparison of range and drift values obtained from six-degree-of-freedom model with and without range wind effect (Aerodynamic jump) on drift and fuzz factor, with corresponding range table values.

Table 4. Comparison of range and drift values obtained from trimmed six-degree-of-freedom model with 5 m/s crosswind and range wind, with corresponding range table values.

ELEVATION (mils)	RANGE (m)			
	WITH 5m/s CROSSWIND		WITH 5m/s RANGE WIND	
	RANGE TABLE	SIX DEGREE MODEL	RANGE TABLE	SIX DEGREE MODEL
84	2149	2192.68	1699	1743.6
114	4688.9	4758.7	4370.6	4398.87
140	6416	6510.32	6206	6271.35
177	8536	8615.98	8445.9	8504.4
217	10271	10338.45	10267	10329.6
348	14368	14396.7	14526	14582
390	15354	15366.9	15549	16196
521	17909	17931.29	18185	18243.6
659	19666	19669.44	19972	20016
811	20400	20446.9	20649	20739.9

ELEVATION (mils)	DRIFT (m)			
	WITH 5m/s CROSSWIND		WITH 5m/s RANGE WIND	
	RANGE TABLE	SIX DEGREE MODEL	RANGE TABLE	SIX DEGREE MODEL
84	-36.91	-63.969	0.78534	0.964
114	-101.03	-143.14	4.123	3.581
140	-144.33	-194.891	5.8901	6.520
177	-193.23	-255.569	12.075	11.581
217	-230.73	-303.077	14.725	17.63
348	-313.7	-415.541	41.819	40.5
390	-335.79	-445.064	44.765	48.510
521	-506.88	-539.547	98.896	76.401
659	-615.91	-639.511	96.205	104.938
811	-741.29	-761.795	150.2.	120.988

factor of 27, there were appreciable improvement in drift predictions. The values of predicted drift in Column 5 of Table 3 matches quite satisfactorily with the range table values. Figure 3 displays the stepwise improvement in range and drift due to range wind at different elevations. In determining the fuzz factor required for trajectory trimming, wind velocity of 10m/s was assumed. In order to check the accuracy of the trimmed model, different trajectories were computed at different elevations assuming constant wind of 5m/s. The results thus obtained are presented in Table 4. The predictions for range and drift for this case are quite satisfactory.

For real life application, usage of these model, becomes cumbersome, inaccurate as these requires extensive trimming using fuzz factor under varied wind conditions. Thus neural model was tried to overcome these difficulties as neural network approach does not require a priori postulation of model.

4.3 Neural Modelling

The data sets generated from the range table were used for the training the neural models. For the purpose of modelling, a set of randomly selected input-output data was selected. Sets of varying number of input-output samples were tried to arrive at the minimum number of samples required for adequate training level. It is realized that in real life the real number of samples available will be limited due to the cost involved in collecting such range data, and hence the need to search for the minimum number of data samples to get an acceptable neural model. The numbers of samples tried were 95,48,30 and 15. Higher number of samples obviously led to better training, but even as few as 15 samples also gave satisfactory models. The suitability of model is tested by a test

(validation) set of data, typically consisting of 30 input-output samples, selected randomly from range table; If the MSE was only of the order of two times the MSE prescribed for the training phase, the neural model was accepted and its architecture fixed for the prediction phase. If not, the architecture was varied till it met the above conditions on MSE for training and validation phase.

Once the neural model is validated, it is used for the prediction purpose. For the prediction, a set of randomly selected data is taken from the range table, and only the input variables of this set are treated as known while the output variable is predicted by the neural model. Since the output is also known from the range table, it is compared with the neural model output to show how well the predicted values compare with the known values. Typically for prediction, 10 samples were randomly selected from the range table.

In case of neural models like Model 1 and Model 2, prediction of more than one output was required, e.g. Model 1 is to predict range and drift. In view of this, the neural models having more than one output were subjected to the following test: for the same set of inputs, is it better to train the network separately for one output at a time, or train it on all the outputs at once. It was observed that even though the latter option gave reasonable predictions of all outputs, the former option always yielded relatively more accurate predictions. The accuracy being of the prime concern, it is worthwhile to have separate neural models for each of the output variables and therefore, all studies repeated herein are based on the single output predictions.

Because the above details of the procedure are common to all the models discussed next, we shall refrain from repeating it and only point out wherever the procedure differs in some significant way from the above mentioned guidelines. Results

for the various models discussed next are presented in tabular as well as in graphical form.

4.4 Model 1

In Model 1, we wish to develop neural model for predicting range (R) and drift (ψ). These would therefore, form the output variables of neural model. These output variables depend on firing angle (θ), change in ballistic air temperature (ΔT), pressure (ΔP), charge temperature (T_c), and head/tail wind (W_x), cross wind (W_y). Thus neural model has R , or ψ as the output variables and θ , ΔT , ΔP , ΔT_c , W_x , W_y as input variables. The W_x and W_y are given in m/s, while ΔT , ΔT_c in °C, and ΔP in mm of Hg.

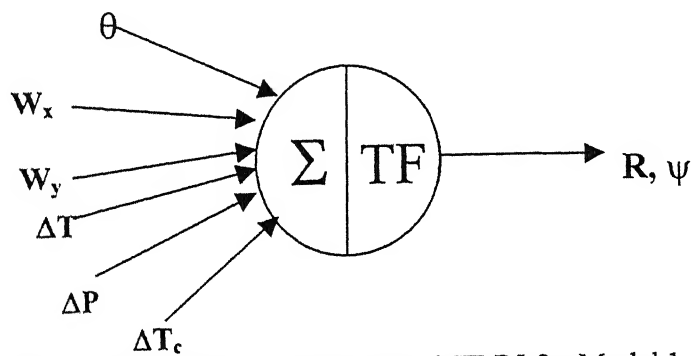


Fig. 5 Schematic representation of FFNN for Model 1

As mentioned earlier, input-output samples were randomly selected from the firing data. Although training was carried out for data sets having 98,48,30,15 samples, the results for the most stringent case of data sets having 15 samples are presented. For the data set having the higher number of samples (>15), the training was always superior to that of 15 samples. Notwithstanding the superior training for the case of 95 samples, for the case of 15 samples, in absolute terms, the training level achieved was satisfactory,

Table 5. Model 1: Comparison of Range Table and Model 1 predicted Range (R) and Drift (ψ) for varying ambient atmospheric Conditions, and charge temperature.

ELEVA-TION (mils)	RANGE		DRIFT			
	RANGE TABLE (m)	MODEL 1 (m)	RANGE TABLE		MODEL 1	
			(mils)	(m)	(mils)	(m)
84	1079	1079	18.421	19.512	18.619	19.722
114	5092.3	5057.3	-43.908	-219.5	-43.899	-219.45
156	7079.2	7126.3	-28.297	-196.65	-28.071	195.08
217	11620	11653	19.121	218.11	19.046	217.26
348	14882	14841	-27.837	-406.68	-31.835	-465.09
416	15392	15326	44.724	675.78	46.571	703.69
521	17683	17608	57.698	1001.6	56.534	981.37
659	19083	18951	-48.54	-909.31	-48.008	-899.35
737	19638	19357	-36.017	-694.34	-38.684	-745.76
811	19891	19891	-39.738	-775.94	-39.749	-776.16

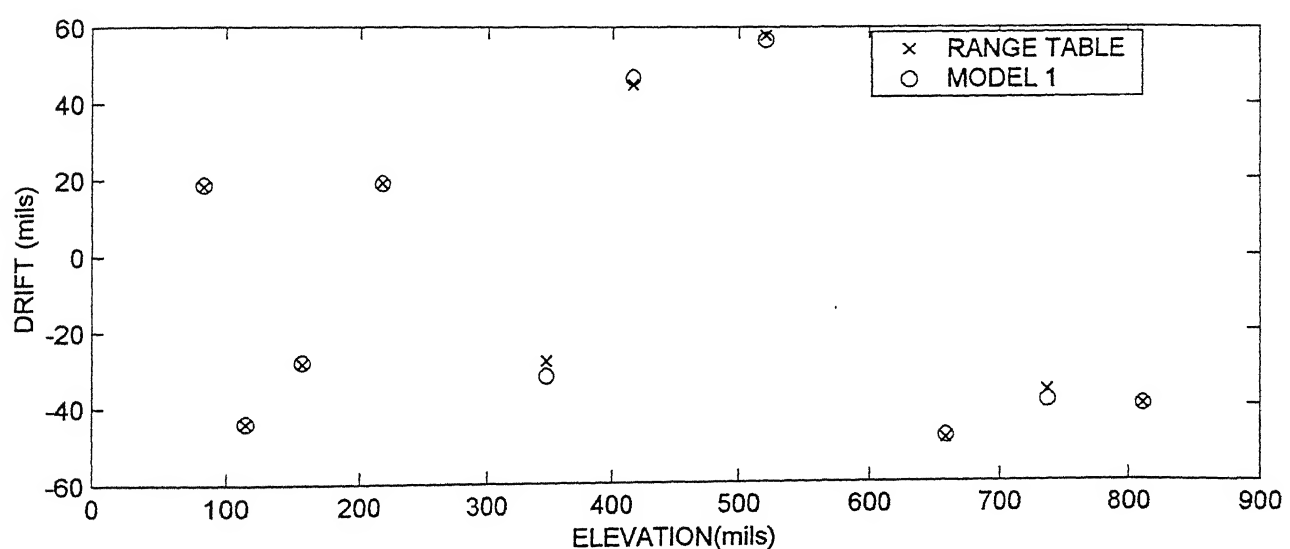
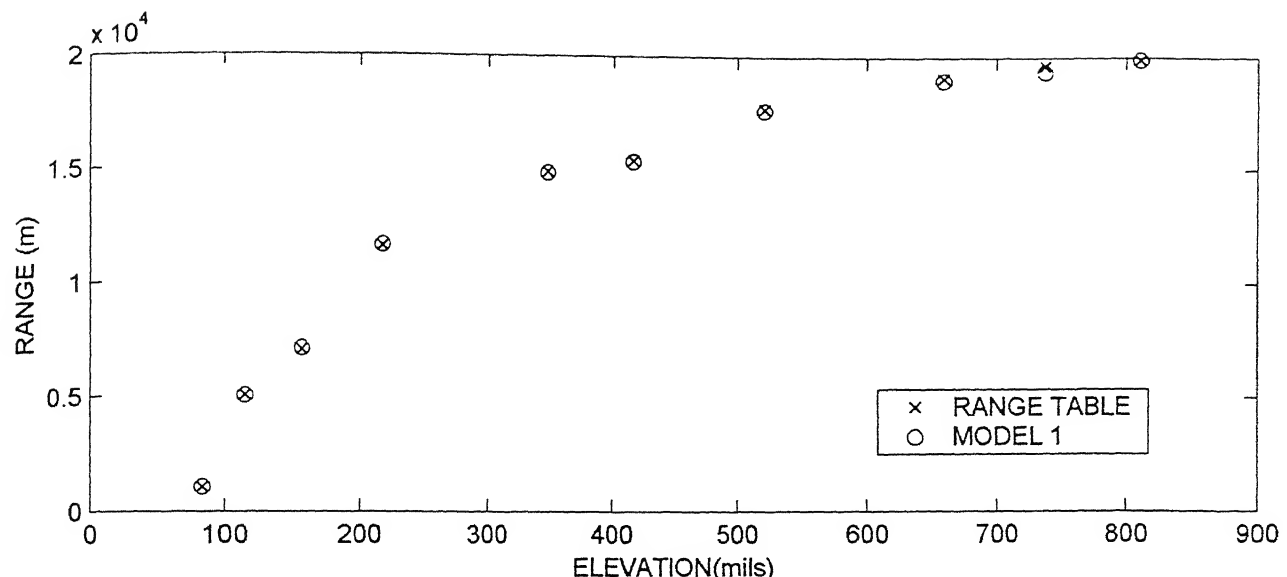


Fig. 6. . Model 1: Comparison of Range Table and Model 1 predicted Range (R) and Drift (ψ) for varying ambient atmospheric Conditions, and charge temperature.

as also was the validation test. Hence, all results presented are only for case of 15 samples.

For randomly selected 15 samples, the corresponding R and ψ were calculated as explained in 4.1. In addition, two other sets of 30 samples each was similarly generated for use as test data. The network tuning parameters were varied till acceptable network training was achieved as per criteria set out in appendix A. New set of 10 samples, randomly taken from the given data was used to predict R , ψ . The results are given in Table 5 and graphically compared with actual values in Fig 6. As may be seen, the predicted values compare well with the actual values.

4.5 Model 2

This model is one, which would be of more use in real life applications. A soldier would want to know the firing angle (θ) he should use, the bearing correction (ψ) he should apply for rocket to reach target. The information made available prior to firing of the rocket is the ambient atmospheric conditions: head/tail wind (W_x), crosswind (W_y), change in air temperature, air pressure, charge temperature. Thus for the desired range under the prevailing atmospheric conditions, we wish to develop a model that would predict the firing angle. The schematic of such model is shown in Fig. 7.

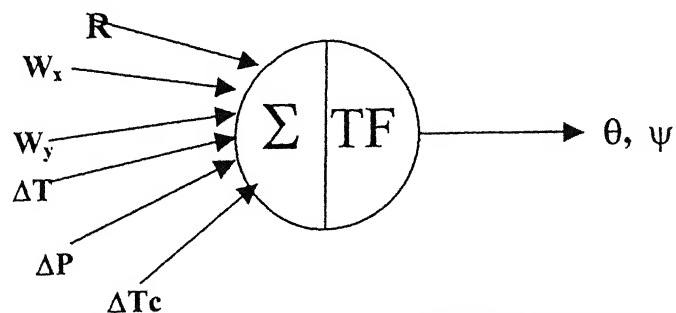


Fig. 7 Schematic representation of FFNN for Model 2

Table 6. Model 2: Comparison of Range Table and Model 2 predicted Elevation (θ) Drift (ψ) for varying ambient atmospheric conditions, and Charge temperature for given range

ELEVATION (mils)	ELEVATION		RANGE		DRIFT	
	RANGE TABLE (mils)	MODEL 2 (mils)	RANGE TABLE (m)	MODEL 2 (m)	RANGE TABLE (mils)	MODEL 2 (mils)
84	84	84.5	1079	1124	18.421	18.481
114	114	113.53	5092.3	5056.2	-43.908	-42.379
156	156	154.94	7079.2	7016.8	-28.297	-28.461
217	217	220.8	11620	11763	19.121	18.195
348	348	355.02	14882	15058	-27.837	-32.128
416	416	423.51	15392	15557	44.724	48.537
521	521	492.24	17683	17223	57.698	53.224
659	659	659.06	19083	19084	-48.54	-44.055
737	737	805.73	19638	19830	-36.017	-38.116
811	811	810.93	19891	19891	-39.738	-39.568

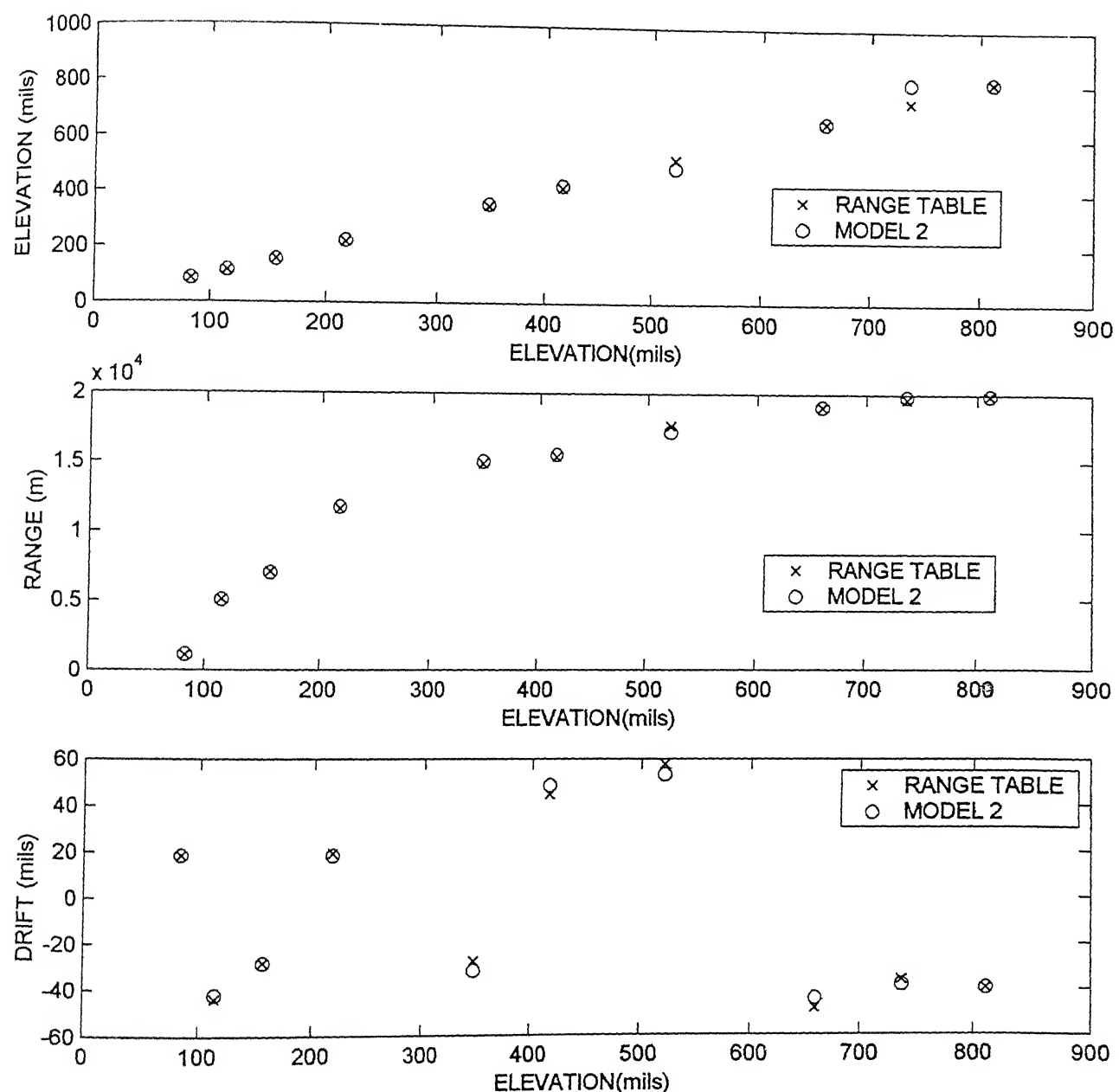


Fig. 8 Comparison of Range Table and Model 2 predicted Elevation (θ)
Drift (ψ) for varying ambient atmospheric conditions, and Charge-
temperature for given range.

The result for Model 2 are shown in Table 6 and Figure 8. The predicted θ , ψ compare well with the actual values, the prediction being marginally better for lower values of θ . One explanation for such observed behavior is the fact that at lower end of θ the range obtainable is more sensitive to variation in θ ; typically, increase of 1 mil result in range increasing by 90m for a nominal value of $\theta = 84$ mils, but at nominal value of $\theta=737$ mils, 1mil increase in θ would result in range increasing by 2.8 m. Notwithstanding this sensitivity of range on nominal value of θ , the predicted value by Model 2 are quite acceptable for the whole range of θ values.

4.6 Model 3

It is of interest to develop a model that can yield standard range (X) obtainable under standard conditions- temperature and pressure corresponding to sea level values in standard atmosphere, no change in charge temperature, no head/tail wind and crosswind. The data assumed to be available for such modelling is measured range (R) for existing ambient temperature, pressure, head/tail wind, crosswind, charge temperature.

Model 3 is identical to Model 1, but it is used in special way for estimating standard range. Like Model 1, output of the network is range, which is mapped to $\theta, \Delta T, \Delta P, \Delta T_c$, head/tail wind W_x , crosswind W_y . However, mapping of the inputs to bearing correction ψ is not required as done for Model 1. The network is trained on 15 data taken from the range table. Now network is used to predict standard range for each of firing angle θ by setting $\Delta T=0, \Delta P=0, \Delta T_c=0, W_x=0, W_y=0$. The standard range for various values of θ so obtained is given in Table 7.

Table 7. Model 3: Comparison of Range Table and Model 3 predicted Standard Range (X) at standard atmospheric for given elevations.

ELEVATION (mils)	RANGE	
	RANGE TABLE (m)	MODEL 3 (m)
84	1600	1657.3
114	4200	4186.1
156	7000	7035
217	10000	10035
348	14200	14135
416	15800	15741
521	17800	17730
659	19600	19399
737	20200	20049
811	20400	20588

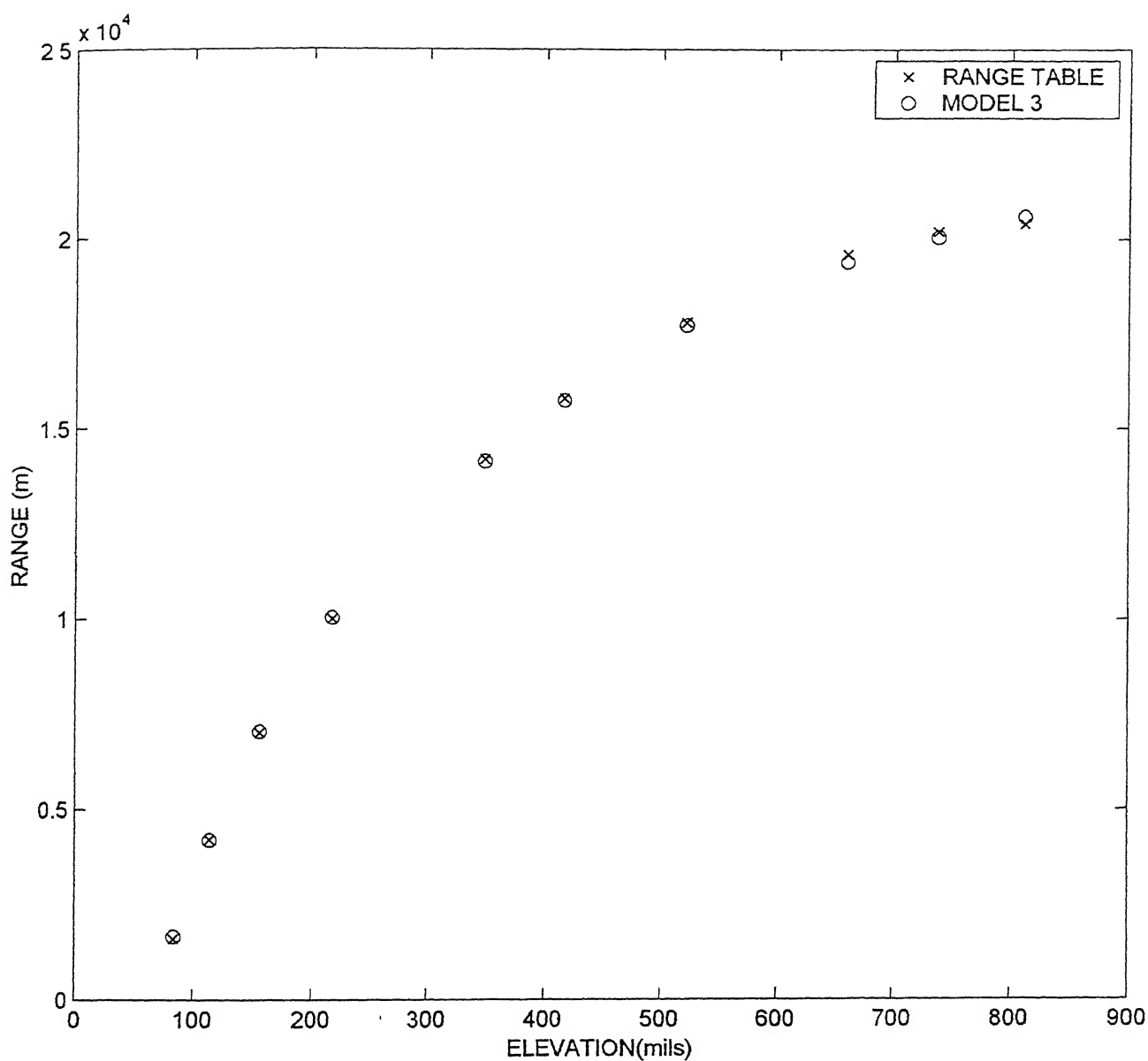


Fig. 9. Comparison of Range Table and Model 3 predicted standard Range (X) at standard atmospheric condition and no change in charge temperature for given elevation.

In Table 7 and Fig 9, the predicted standard X via Model 3 are compared with that from the range table. Though model gives standard X which compare well with that given by the range table, it is observed that prediction for standard range are relatively better for lower valued of θ , i.e. there is slight decrease in prediction accuracy of standard R as θ increases.

CHAPTER 5

CONCLUSION

5.1 Conclusions

The validity of the neural modeling is demonstrated for three different applications relevant for artillery rocket. A set of available firing data in terms of range, firing angles, existing atmospheric conditions like temperature, pressure, head/tail wind, cross wind, charge temperature, are required to train the network with suitable input-output samples which of these measured variables would form the inputs and the outputs is decided by the purpose of the neural model. In particular, for three distinct applications, a neural model has been identified and validated for Grad-rocket data. The results for all the models compare well with the known results. The strength of the neural models lies in the fact that once the network is trained, it can be used for on-line applications on the field of action-to predict the range for chosen angle of firing or to predict the firing angle for desired range, under the prevailing atmospheric conditions and for known charge temperature.

The conventional approach i.e., the mathematical model such as six-degrees-of-freedom model requires knowledge of all the forces and moments acting on the rocket. Evaluation of forces and moments, in turn, require aerodynamic coefficients as inputs and this fact limits the accuracy of predictions because the reliability of available estimates of these coefficients is not always high. In contrast, the proposed neural models do not require any mathematical model or its solution. This implies that the neural models do not require estimates of aerodynamic coefficients. Furthermore, if the neural network is

trained on the real data, it will automatically account for the initial conditions in an implicit way. But the mathematical models have no provisions to account for initial conditions such as tip-off and aerodynamic jump.

5.2 Suggestion for Future Work

- 1) The training of the neural network depends on the architecture of the FFNNs, the activation function used by the neurons and the values selected for the tuning parameters. From the neural network point of view, lot of scope exists to explore and experiment with new evolving schemes and methodologies for improving the input-output mapping.
- 2) The present work has used the firing tables provided by ARDE, Pune. An attempt should be made to seek real firing data and validate the present models for such data.
- 3) The data set supplied by ARDE, Pune is valid for weighted value of the head/tail wind and cross wind. This is an approximation to varying wind conditions at different altitudes through which the rocket passes. It may be worthwhile to search for a way to account for varying wind conditions. The same comment also applies for finding a way to account for varying temperature and density conditions.

REFERENCES

1. Anonymous, "Engineering Design Handbook Series of the Army Material Command," AMCP-706-280, US Army, North Carolina, June 1970.
2. Anonymous, "Text-Book of Ballistics and Gunnery (TBBG)," Vol. 2, HMSO, London, 1987.
3. Haykins, S. "Neural Networks - A Comprehensive Foundation," McMaster University, McMillan College Publishing Company, New York, 1994.
4. Hopfield, J. J., "Neural Networks and Physical Systems with Emergent Collective Computational Abilities," Proceeding of the National Academy of Sciences, Vol. 79, 1982, pp. 2254-2558.
5. Hornik, K., Stinchcombe, M., and White, H., "Multi layer Feed Forward Network are Universal Approximators," Neural Networks, Vol. 2, No. 5, 1989, pp. 359-366.
6. Bassapa, and Jategaonkar, R. V., "Aspect of Feed Forward Neural Network Modelling and its application to Lateral-Directional Flight Data," DLR-IB 111-95/30, Braunschweig, Germany, Sept. 1995.
7. Hess, R. A., "On the Use of Back Propagation with Feed Forward Neural Networks for the Aerodynamic Estimation Problem," AIAA paper 93-3638, August. 1993.

8. Linse, D. J., Stengel, R. F., "Identification of Aerodynamic Coefficients Using Computational Neural Networks," Journal of Guidance, Control, Dynamics, Vol. 16, No.6, 1993, pp. 1018-1025.
9. Raisinghani, S. C., Ghosh, A. K., and Kalra, P. K., "Two new Techniques for Aircraft Parameter Estimation Using Neural Networks," The Aeronautical Journal, Vol.102, No.1011, 1998, pp. 25-29.
10. Ghosh, A. K., Raisinghani, S. C., and Khubchandni, S., "Estimation of Aircraft Lateral-Directional Parameters via Neural Networks," The Journal of aircraft, Vol.35, No.6, 1998, pp. 876-881.
11. Ghosh, A. K., and Raisinghani, S. C., "Frequency - Domain Estimation of Parameter From Flight Data Using Neural Network," to appear in Journal of Guidance, Control and Dynamics, Vol.24, No.2, March-April 2001.
12. Ghosh, A. K. and Raisinghani, S. C., "Parameter Estimation From the Flight Data of an unstable aircraft using Neural Networks," AIAA, pp. 405-411.
13. Raisinghani, S. C., Ghosh, A. K., "Parameter Estimation of an Aeroelastic aircraft using Neural Networks," Sadhana, Vol.25, Part 2, April 2000, pp. 181-191.

14. Dehury, S. K., "Modelling of Performance Artillery Shell using Neural Networks," M. Tech Thesis, IIT Kanpur, India, December 2000. April 1998.

15. Maine, R. E. and Illif, K. W., "Application of Parameter Estimation of Aircraft Stability and Control: The Output-Error Approach, NASA Reference Publication 1168, 1986.

16. Krishnamuthy, K and Selvarajan, S., "Wind Tunnel Test Results on Rocket (RG-122) Model in the Mach Number Range 0.6 to 3.0," NAL TWT, 4-107-84, December 1984.

Appendix A

FEED FORWARD NEURAL NETWORK

The back propagation network consists of one input layer, one output layer and one or more hidden layers. There is no theoretical limit on the number of hidden layers but typically there is just one or two. Some work has been done [14], which indicates that minimums of four layers (three hidden layers and one output layer) are required to solve problems of any complexities. Each layer is fully connected to the succeeding layer (standard connection).

There are as many neurons in the input layer as there are inputs, and likewise with the output layer. The number of layers and the number of neurons in the hidden layers(s) must be determined by trial and error. There is no quantifiable best answer to the layout of the network for any particular application. There are only general rules picked up over time and followed by most researchers and engineers applying various architectures to their problems.

Rule 1. As the complexities in the relationship between the input data and the desired output increases, the number of processing elements in the hidden layer should increase.

Rule 2. If the process being modeled is separable into multiple stages, then additional hidden layers may be required. If the process is not separable into stages, then additional layers may simply enable memorization and not a true general solution.

Rule 3. The amount of available training data sets an upper bound for the number of processing elements in the hidden layer. To calculate this upper bound, use the

number of input-output pair examples in the training set and divide that number by the total number of input and output processing elements in the network. Then divide the result again by a scaling factor between five and ten. Larger scaling factors are used for noisy data. Extremely noisy data may require a factor of twenty or even fifty. Very clean input data with an exact relationship to the output might allow the factor to be dropped to around two.

Cross-Validation and Overtraining

One approach to avoid over-training of the network is to estimate the generalization ability during training and stop when it begins to decrease. The essence of back-propagation learning is to encode an input-output relation, presented by a set of data, with a multiplayer perceptron well trained in the sense that it learns enough about the past to generalize to the future. The simplest method is to randomly partition the data set into a training set and test (validation) set. From the training set, a validation subset, which are typically 10 to 20 percent of the training set is set aside. The motivation here to validate the model on a data set different from the training set that is used for selecting the architecture of the network. The training set is used to modify the weights, the validation set is used to estimate the generalization ability. The architecture of the network is varied till the training set results in MSE less than the prescribed value ε . This architecture is now tested on the test data (which can be one or more) and if the MSE is of the order of 2ε , the architecture is accepted to yield the desired neural model and assumed to be capable of predicting required output for inputs not seen earlier by the network.

Another way of avoiding over-training is to limit the ability of the network to take advantage of spurious correlation in the data. Over fitting is thought to happen when the network has more degree-of-freedom (the number of weights, roughly) than the number of the training samples when there are not enough examples to constrain the network. Even though it may give exactly right output at the training points, it may be very inaccurate at other points. An example is a higher order polynomial fitted through a small number of points.

Sufficient Training Set Size for a Valid Generalization

Generalization is influenced by three factors: i) the size and the efficiency of the training set, ii) the architecture of the network, and iii) the physical complexities of the problem at hand. Clearly, we have no control over the last factor, i.e. the physical complexity. We have already discussed the choice of architecture based on training and test data. Once the architecture of the network is fixed, then the size of training set can be derived as follows:

Let M denote the total number of hidden layer computation nodes. Let W and N be the total number of synaptic weights and the number of random examples used to train the network respectively. Let ε denote the fraction of error permitted on test. Then, according to Baum and Haussler, [2] the network will almost certainly provide generalization provided the following two conditions are met.

- (a) The fraction of error made on the training set is less than $\varepsilon/2$.
- (b) The number of examples(N) used in the training is

$$N \geq 32 \frac{W}{\varepsilon} \ln \frac{W}{\varepsilon}$$

where W is the total number of synaptic weights.

Ignoring the logarithmic factor, taking first order approximation, the number of training examples is directly proportional to the number of weights in the network and inversely

proportional to the accuracy parameter ε . Then, $N > \frac{W}{\varepsilon}$.

A 13790

137901

Date Slip

The book is to be returned on
the date last stamped.



A137901